



U K A E A

Report

ELECTRON CYCLOTRON RESONANCE
HEATING AT CULHAM
Contributions to the ECRH Workshop,
Brussels, June 1982

W. H. M. CLARK
J. HUGILL
C. N. LASHMORE-DAVIES
M. O'BRIEN
A. C. RIVIERE
D. C. ROBINSON
D. F. H. START
R. A. CAIRNS
J. OWEN

CULHAM LABORATORY
Abingdon Oxfordshire

1982



© - UNITED KINGDOM ATOMIC ENERGY AUTHORITY - 1982
Enquiries about copyright and reproduction should be addressed to the
Librarian, UKAEA, Culham Laboratory, Abingdon, Oxon. OX14 3DB,
England.

ELECTRON CYCLOTRON RESONANCE HEATING AT CULHAM
Contributions to the ECRH Workshop, Brussels, June 1982

W H M Clark, J Hugill, C N Lashmore-Davies, M O'Brien
A C Riviere, D C Robinson and D F H Start

Culham Laboratory, Abingdon, Oxon OX14 3DB, UK
(Euratom/UKAEA Fusion Association)

R A Cairns and J Owen

University of St Andrews

ABSTRACT

This paper describes the main features of the present Culham programme of ECRH experiments and theoretical work, how this programme may develop in the future and the corresponding requirements in terms of frequency, power and pulse length of gyrotron power sources.

May 1982

LIST OF CONTENTS

	Page
1 INTRODUCTION A C Riviere	1
2 BETA OPTIMISATION ON CULHAM TOROIDAL FACILITIES USING ECRH D C Robinson	3
3 ECRH DRIVEN CURRENTS IN TOSCA, CLEO AND COMPASS D F H Start and M O'Brien	11
4 USES OF ELECTRON CYCLOTRON RESONANCE HEATING ON DITE W H M Clark and J Hugill	19
5 CURRENT DRIVE AND PROFILE CONTROL WITH ECRH ON DITE C N Lashmore-Davies, R A Cairns and J Owen	25
6 GYROTRON NEEDS AND WAVEGUIDE COMPONENTS A C Riviere	31

1 INTRODUCTION

by A C Riviere

Electron cyclotron resonance heating (ECRH) of toroidal plasmas has several attractive features compared with other rf heating schemes. Only a simple antenna is required and this can be located well away from the plasma edge, neither the wave propagation nor the absorption is affected by the edge plasma and the power is absorbed locally in the region where the cyclotron resonance condition is satisfied for a wide range of plasma conditions. Also, progress in the use of ECRH has been very encouraging. Experiments in the USSR^[1], USA^[2], Japan^[3] and the UK^[4] have shown efficient absorption of the wave power and no apparent deterioration in energy confinement. These are good reasons for more extensive use of ECRH for additional heating and for strong support of the development of appropriate high frequency gyrotrons.

There are several important questions still to be answered regarding the suitability of the tokamak as a DT burner for a fusion power plant, namely the possibility of a beta limit, the occurrence of disruptions, rather poor energy confinement and pulsed operation. The first three of these are relevant to the success of JET, NET and INTOR. At Culham these questions are being studied on the TOSCA, CLEO and DITE experiments and, in the future, on COMPASS. ECRH can be used to advantage in these devices for additional heating, profile control and current drive in support of this programme. The ECRH activity at Culham is seen as an important element in studies aimed at the further development of the tokamak concept. In addition the programme includes studies in CLEO operated as a stellarator. Detailed discussion of the programme is given in Sections 2, 3, 4 and 5 below and the gyrotron needs are discussed in Section 6.

2. BETA OPTIMISATION ON CULHAM TOROIDAL CONFINEMENT FACILITIES USING ECRH

by D C Robinson

2.1 INTRODUCTION

The limiting value of beta is of particular importance to the ultimate potential of a tokamak as an economic reactor. It is very important to obtain an experimental indication whether beta values of 5% or more are attainable in a tokamak without a strong decrease in confinement. If the limit is close to that achieved so far (about 2%) then the next generation devices such as INTOR, NET and FED and reactors are technically implausible. The success of JET is also dependent on the attainment of high values of beta. With additional heating the TOSCA, CLEO and DITE experiments and the proposed COMPASS device are well suited for such experiments.

Average values of beta in the tokamak obtained experimentally in this laboratory have ranged between 1 and 2%. 1% has been obtained with high power neutral injection on the DITE tokamak^[5]. 2% has been obtained by gas puffing and decompression of an ohmically heated plasma on TOSCA^[6]. A value of 1% has been obtained by ECRH at the second harmonic on TOSCA with a value of poloidal beta equal to the aspect ratio^[7]. There is no clear indication in these experiments that the average value of beta conforms with the limiting values predicted from ideal MHD theory for such experiments. The 3 tokamaks which are available to us at present are TOSCA, with an aspect ratio of 3.5, DITE with an aspect ratio of 4.5 and CLEO with an aspect ratio of 7 - see Table 2.1. As the optimised value of beta from ideal MHD calculations scales as $(a/R)^{3/2}$ ^[8] then the optimum beta values from theory for these different experiments vary by a factor of three.

We can estimate the power to reach a critical value of beta in these different devices by using one of the measured scaling laws for the gross electron energy confinement time^[9]

$$\tau_{E_e} \cong 3.6 \times 10^{-19} \bar{n}_e a^2 q^{3/4} \quad (\text{c.g.s.})$$

and inserting the maximum line average density for accessibility of the rf power at the particular gyrotron frequency for the second harmonic or fundamental. These initial energy confinement times for the ohmically heated plasmas are shown in column 3 of Table 2.1 for the different devices for $q=3$. However at low densities the measured confinement times on TOSCA and CLEO are a factor of two higher than that which this empirical scaling law predicts though the value for DITE

is close to correct. If we assume that the critical beta is proportional to $\frac{a}{Rq^2}$, which gives the numbers shown in column 2 of Table 21 for $q=3$, then if the confinement does not decrease with ECRH (for which there is evidence from a number of experiments) the power to reach the critical beta is proportional to $a/q^{2.75}$. The actual values for circular and non-circular plasmas are given in column 6 of Table 21 using the experimental values of τ_{Ee} . The power is independent of the frequency but operation at the fundamental requires twice the power unless the extraordinary mode is used from the inside.

From Table 21 it is clear that critical beta studies can be conducted on the first two devices at modest power levels at the second harmonic provided the incident power is absorbed efficiently. Column 7 shows the percentage absorption for a single pass for the different devices at the second harmonic and fundamental. At the second harmonic at 60 GHz the absorption exceeds 80% on three of the four devices. Ray tracing calculations show that even at 28 GHz on TOSCA the absorption reaches 50%. Allowing for wall reflections Fielding^[10] has shown that the heating efficiency exceeds 50% and this has been verified experimentally^[7].

As second harmonic electron heating rates increase with the kinetic energy transverse to the magnetic field, there is a maximum heating rate beyond which collisions are incapable of maintaining a thermal electron distribution^[10,11]. For the power required to reach the critical beta at 60 GHz this is not a problem (except possibly very locally). As the threshold is proportional to f^2 (f is the frequency) then this is expected to be a problem at high powers on TOSCA and CLEO at 28 GHz. This occurs at a power level of 250 kW when the temperature exceeds 1 keV on TOSCA. This effect is likely to lead to a build up in the trapped electron population which may have consequences for confinement and stability.

ECRH can be used to optimise the value of beta in these devices in three ways.

(a) Bulk heating. The small size of the TOSCA device gives it a significant advantage in that the critical beta values (particularly at high q) can be reached with modest amounts of radio frequency power ≈ 200 kW as the absorption is $> 50\%$ after allowing for wall reflections^[7,10]. The power to reach the critical beta value is observed to be less than that given in the Table as the confinement time is observed to improve.

(b) Profile Control for Low q. A great virtue of ECRH, as it can deposit power locally, is its potential ability to control the temperature profile and thereby on a local field diffusion timescale, the current profile. This has not yet been fully demonstrated experimentally. An alternative method to control the current profile is to directly drive current, see Section 4. In principle this would permit optimisation of the current profiles and thereby the value of beta. It should permit access to low q (< 2) operation, by controlling the $m=2$ mode, which increases the value of beta, and the control or minimisation of the effects of disruptions. The power needed to control the $m=2$ mode is shown in Table 2.1, column 8. This has been obtained by using a two dimensional calculation for the electron energy balance with anomalous losses and field diffusion with a localised heating source^[12]. Figure 2.1 is a typical result for the TOSCA device. The resultant current profile is then checked against resistive instability calculations for the $m=2$ tearing mode^[13].

(c) Profile Control for Non-circular Plasmas. Of particular relevance to JET, is the optimisation of a non-circular tokamak which could be achieved with ECRH. Calculations are being carried out to verify if profile control can be effected more efficiently using current drive rather than by heating and current diffusion.

2.2 TOSCA

This device has already obtained high average values of beta with ohmic heating alone, 1-2%^[6]. Further investigations with ECRH have been made to determine if these values are limiting or not^[7]. Detailed experiments to date to look for ballooning modes of either resistive or ideal MHD origin have failed to reveal a detailed correlation with beta^[13]. Future experiments to be conducted on this device are as follows:

(a) ECRH at the second harmonic with strong absorption per single pass has already produced discharges with $\beta_0 \sim R/a$ for high q (~ 5) discharges where the limiting value of beta is relatively low ($\sim 1\%$). As the discharge evolves as a flux conserving tokamak for 3 ms these experiments require longer times and more power to be definitive. The longer time is required because at the conductivity temperatures obtained the heating pulse at present (3 ms) is shorter than the field diffusion time (~ 10 ms).

(b) Heating experiments on non-circular plasmas. To date no improvement in the value of beta has been obtained on TOSCA or any other device with non-

circular plasmas. Attempts at profile control with non-circular plasmas will be made.

(c) Current drive experiments have produced up to 30% of the plasma current driven by cyclotron waves^[7]. Attempts will be made to increase this percentage further and to see if this can be used to provide profile control.

(d) Profile control should make it possible to produce low q discharges (< 2) which can produce high average values of beta. This has already been achieved on the TOSCA device using saddle coil windings for instability control. It is observed experimentally using ECRH for low q experiments on the TOSCA device that an excessive streaming parameter leads to poor absorption efficiency^[7]. This is difficult to avoid as low q operation requires high currents and low densities necessary for access for the 28 GHz radiation. The streaming parameter ($\xi = v_D/c_s \sim j/nvT \sim B_\phi/RnvT$) is improved considerably ($\sim 3 \times$) by operating at 60 GHz.

The requirements for this radio frequency heating programme on the TOSCA device are :- pulse lengths of up to 10 ms with power levels in excess of 200 kW at 28 GHz and for operation at lower values of q and higher densities - 200 kW at 60 GHz.

2.3 CLEO

This device has an aspect ratio of 7 and has a close fitting conducting wall with a time constant of $3\frac{1}{2}$ ms which is smooth and very close to the plasma. It can produce much longer pulse lengths than the TOSCA device typically up to 100 ms. The key experiments planned here are:

(a) To compare ECRH at the second harmonic with that on TOSCA where the absorption per single pass is two times larger than that of TOSCA and the streaming parameter is three times smaller. Limiting beta studies should be possible because the aspect ratio is now 7 and the critical beta value can be reached with a power input in excess of 400 kW (Table 2).

(b) As the radio frequency power absorption should be better than on TOSCA and the pulse length is longer, further profile control experiments will be possible, in particular low q access by ECRH. Low q access has already been demonstrated in ohmic heated discharges. It may also be possible to demonstrate disruption control on this device.

(c) ECRH experiments to obtain high values of beta will take place on CLEO with near stellarator-like operation when the ohmic heating current is small. Then the efficiency of ECRH may well be higher than in a tokamak. Heating experiments will be performed on stellarator and hybrid stellarator configurations (HALQT). A comparison of the results with Wendelstein VIIA ($\ell=2$) should be interesting.

(d) Long pulse operation on the CLEO device will permit further tests of current drive on this larger facility. By using the helical windings clearer evidence will be obtained for sustained current drive on this facility, than is possible on a tokamak.

The requirements for this programme are for radio frequency heating pulses of up to 100 ms at power levels of up to 400 kW (not simultaneously) at 28 GHz and also 100 ms at 60 GHz for low q investigations at higher densities.

2.4 DITE

As on other tokamaks with high power neutral injection the DITE device exhibits a decrease in confinement which leads to a modest value of β ($\lesssim 1\%$). It is proposed to perform a set of heating experiments which will use both neutral injection and electron cyclotron resonant heating to provide more independent control of the electron temperature profile to ascertain if this will improve the efficiency of neutral beam heating and thereby the value of beta. A 60 GHz gyrotron will be used at the fundamental frequency where an absorption of 80% should be obtained (Table 21). At power levels of 200 kW this will perturb the electron temperature profiles and may assist in beta optimisation. Later it is proposed to increase the power to fully support the electrons during neutral injection. Fields and antenna systems similar to those that could be used on JET would be used. Further investigations including current drive and profile control with ECRH at the second harmonic on DITE have also been considered, see Section 5.

2.5 COMPASS

A new device of moderate size ($a=22$ cm, $b=33$ cm, $R=55$ cm, $I_p \lesssim 200$ kA, $B_{\phi} \lesssim 1.2$ T) has been proposed to explore the MHD optimisation of tokamaks. This involves low q operation (< 2) using local ECRH and/or mode control. Both passive and active control of instabilities will be possible and together with

current profile control this should permit control of disruptions. Beta optimisation of a tokamak is possible through low q operation, profile control, and by the use of a non-circular cross section. Long pulse operation (seconds) using electron cyclotron waves to drive the plasma current may be possible. It is proposed to use initially the existing gyrotrons to heat and control the non-circular plasma (0.6 MW) and then to use 2 MW of ECRH at 60 GHz to produce high beta plasmas ($\beta > 5\%$).

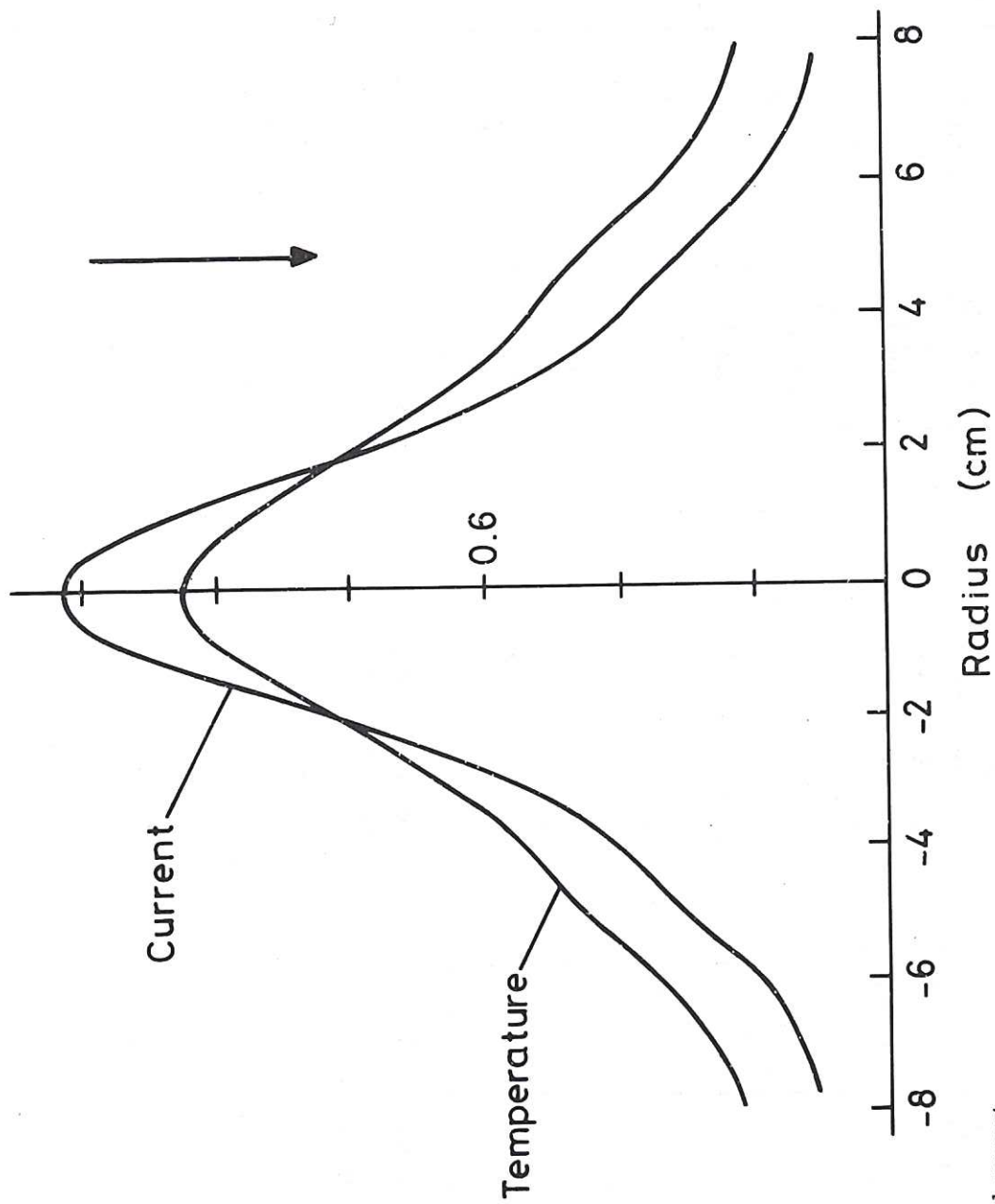
CONCLUSIONS

A significant programme on critical beta studies in tokamaks and an $\ell=3$ stellarator can be conducted on the TOSCA, CLEO and DITE facilities using ECRH. To conduct part of the programme of heating and control on the TOSCA/CLEO devices requires the existing gyrotrons but with an enhanced power supply. Operation at higher densities and thereby smaller streaming parameters and stronger absorption per single pass can be achieved by using a higher frequency gyrotron (60 GHz). Long pulse current drive experiments will be attempted on both TOSCA and CLEO. Experiments on the DITE device using both neutral injection and ECRH should be valuable in elucidating the reasons for beta limitations on NI and may lead to further beta optimisation in that heating scenario. The proposed tight aspect ratio COMPASS device will add significantly to limiting beta investigations in the future.

Table 2.1

Device	R/a	$\bar{\beta}_C$ (%) [1]	Empirical τ_{Fe} (ms)		Experimental τ_{Fe} (ms)	Harmonic	Power to β_C (kW)	% Absorption/pass	Power to control $m=2$ (kW)
			28 GHz	60 GHz					
TOSCA	3.5	2.4	0.16	-	0.4	2	345 [3]	30 [2]	30
			-	0.64		2		53	
CLEO	7	1.2	0.42	-	1.0	2	547 [3]	62	40
			-	1.6		2		91	
			-	4.0		1		70	
COMPASS	2.5	3.3 (6.0)	-	6	-	2	1,444	80	150
			-	8		2		2,212	
DITE	4.5	1.9	-	16	-	1	4,425	96	200
			-	-		1		78	

[1] For $q=3$, figures in brackets are for non-circular cross sections
 [2] Ray tracing gives significantly higher values
 [3] Using experimental τ_{Fe}



(Temperature and current
in normalised units)

Fig.2.1 Current and temperature profiles $7 \mu\text{s}$ after switch on of ECRH at $r=5 \text{ cm}$ with $P_f \sim \frac{1}{2} P_{OH}$. Current gradient control is established in $< 100 \mu\text{s}$.

3. ECRH DRIVEN CURRENTS IN TOSCA, CLEO AND COMPASS

D F H Start and M O'Brien

3.1 INTRODUCTION

During the last few years there has been a growing interest in developing non-inductive methods of driving the plasma current in a tokamak with a view to facilitating the continuous operation of a tokamak reactor. One such method, proposed by Fisch and Boozer^[14] in 1980, relies on using Doppler shifted electron cyclotron waves to heat the electron distribution asymmetrically. Experimental verification of these ideas has been obtained in recent ECRH experiments on the Levitron^[15] and TOSCA^[7] devices. However the efficiencies observed in these experiments were low (~ 0.03 A/W) due mainly to the low plasma temperature and small size of the machines, both of these factors conspiring to produce small single pass absorption. In this paper we show (a) how the TOSCA results are understood and can be improved upon, (b) that ECRH can be used on the CLEO device to produce a large fraction of the plasma current and (c) how effective this method is for driving current in COMPASS. The calculations were performed using a ray tracing code together with the full Fokker Planck theory of ECRH current drive developed by Cordey et al^[16]. Electron trapping effects are also considered^[17]. In the various schemes investigated the rays were injected either from the outside of the machine (low field side) at a point on the median plane with co-ordinates $(r, \theta, \phi) = (a, 0, 0)$ or from the inside of the torus (high field side) at a point $(r, \theta, \phi) = (a, 135, 0)$. The co-ordinate system is shown in Fig.3.1 and a is the limiter minor radius. The dependence of the current drive efficiency on injection angle was investigated by varying the angle $\psi = \tan^{-1}(k_\phi/k_r)$ whilst keeping $k_\theta = 0$. The plasma density (n_e) and temperature (T_e) profiles were taken to be of the form $n_e(r) = n_e(0)[1-(r/a)^2]$ and $T_e(r) = T_e(0)[1-(r/a)^2]$ and the sensitivity of the current drive to $T_e(0)$ was also investigated.

3.2 TOSCA

The experiments on TOSCA have so far been carried out with second harmonic ($\ell=2$) ECRH at 28 GHz with the microwave power injected from outside the torus on the median plane. Figure 3.2 shows the calculated single pass power absorption and current drive efficiency for the X mode as a function of the angle of injection (ψ) for a central density $n_e(0) = 4 \times 10^{18} \text{ m}^{-3}$ and temperature $T_e(0) = 500 \text{ eV}$.

The discontinuity at $\psi=14^\circ$ is caused by rays being intercepted by the inner wall of the torus for $\psi < 14^\circ$. Between $\psi=14^\circ$ and $\psi=22^\circ$ the rays are refracted so as to miss the inner wall and make a double pass through the resonance. In this region the current flows in opposing directions on opposite sides of the resonance and so the net current on a given flux surface can be either parallel or antiparallel depending on which component dominates (see Fig.3.3). This effect is responsible for the reversal of the total current between $\psi=15^\circ$ and $\psi=22^\circ$. Above $\psi=22^\circ$ the rays do not cross the resonance and so the absorption and the current fall sharply with increasing angle.

The oppositely directed current channels can be seen in Fig.3.3. where the current profiles were generated by a cone of rays of semi-angle 10° centred about $\psi=14^\circ$ and $k_\theta=0$. The magnitude of the current at 500 eV is close to that observed in the experiment^[7] but this agreement is somewhat fortuitous since the current is very sensitive to the electron temperature. As shown in Fig.3.3 a two-fold increase in T_e produces a six-fold increase in current. This sensitivity results from the cancelling effects of the two current channels. As the temperature is increased the absorption improves and preferentially enhances the current in the outer channel which produces a relatively large change in the net current.

For the case shown in Figs. 3.2 and 3.3 the effect of electron trapping is to dramatically reduce the current. However the reduction is much less if the resonance is placed inside the magnetic axis^[17] and the sensitivity to resonance position could provide a convincing demonstration of the existence of trapping. Some preliminary experimental evidence of this effect has been obtained on TOSCA^[7].

3.3 CLEO

For CLEO we have considered both 28 GHz X-mode fundamental ($\ell=1$) electron cyclotron waves injected from the inside of the torus and 28 GHz X-mode second harmonic waves injected from the outside. Ray trajectories for the X-mode fundamental are shown in Fig.3.4 for $n_e(0) = 10^{19} \text{ m}^{-3}$, $T_e(0) = 200 \text{ eV}$ and a resonance position chosen to place the maximum of the current density profile close to the magnetic axis. The dependence of the current on injection angle is shown in Fig.3.5. The increase in current as the injection angle increases is due to (a) the increased absorption resulting from the ray travelling further at small angles to the field lines (the absorption increases strongly as the angle to the field decreases^[18]) and (b) a larger fraction of the power being absorbed far from the resonance by electrons with high parallel velocity, v_{\parallel} (the current density per unit power density scales as $(v_{\parallel}/v_e)^2$ - see ref [16]).

The current profiles are shown in Fig.3.6 for a cone of rays of semi-angle 10° centred on $\psi=55^\circ$. As in the case of TOSCA the current increases rapidly with T_e as is also shown in Fig.3.7. The reduction due to electron trapping is small due partly to the large aspect ratio of CLEO and partly due to the fact that most of the absorption occurs on the inside of the magnetic axis (see ref [17]).

For the study of the second harmonic injected from the low field side the density $n_e(0)$ was reduced to $4 \times 10^{18} \text{ m}^{-3}$ to avoid the low density cut-off. The variation of absorption and current with injection angle is shown in Fig.3.8. For $\psi < 21^\circ$ rays strike the inner wall of the torus. The sharp maximum in the current corresponds closely to rays glancing the resonance while for $\psi > 22^\circ$ both the absorption and current drop sharply as the refraction keeps the rays away from the resonance. The absolute magnitude of the current is substantially less than for the X-mode fundamental. The narrow radial current profiles and strong T_e dependence are shown in Figs.3.9 and 3.10.

3.4 COMPASS

For this device we compare 28 GHz X-mode fundamental RF injected from the high field side with 60 GHz X-mode second harmonic RF injected from the low field side. The density $n_e(0)$ was taken to be 10^{19} m^{-3} . The results of the calculations are similar to those for CLEO and are shown in Figs.3.11-3.16. However the increased current drive efficiency of the fundamental over the second harmonic is not so marked as in the CLEO case. This is due to the larger aspect ratio of COMPASS which allows the $\ell=1$ rays to bend further towards perpendicular propagation near the resonance thereby reducing the attenuation coefficient.

3.5 SUMMARY

The magnitude of the ECRH driven current on TOSCA is consistent with the ray tracing code calculations. In the near future this code is to be combined with codes which solve the field diffusion equation to facilitate comparison of the observed and predicted loop voltages. The current in TOSCA is predicted to be sensitive to electron trapping and so further experiments are planned to investigate this effect.

For CLEO the scheme utilising X-mode electron cyclotron waves at the fundamental frequency injected from the high field is by far the most efficient for driving current. By operating CLEO in a near stellarator configuration with small ohmic heating current and by extending the gyrotron pulse length to 100 ms it should be possible to obtain a clear demonstration of prolonged ECRH current

drive. The combined ray tracing/field diffusion code will be used to interpret the results. In addition this code provides an electron energy balance analysis so that measurements of χ_e , in particular its dependence on the drift parameter, can be made at the same time as the current drive studies.

For COMPASS, the X-mode fundamental scheme is about 1.5 times more efficient than that based on the second harmonic at $T_e(0) = 1$ keV provided electron trapping is absent. Under these conditions, and at a density $n_e(0) = 10^{19} \text{ m}^{-3}$, over 100 A/kW should be attainable. Should electron trapping be important the 60 GHz second harmonic scheme is preferable. which would give over 50 A/kW.

The ray tracing code used in this work is presently being modified to incorporate the full relativistic resonance condition given by Cairns et al [19] and this should improve the current drive efficiencies.

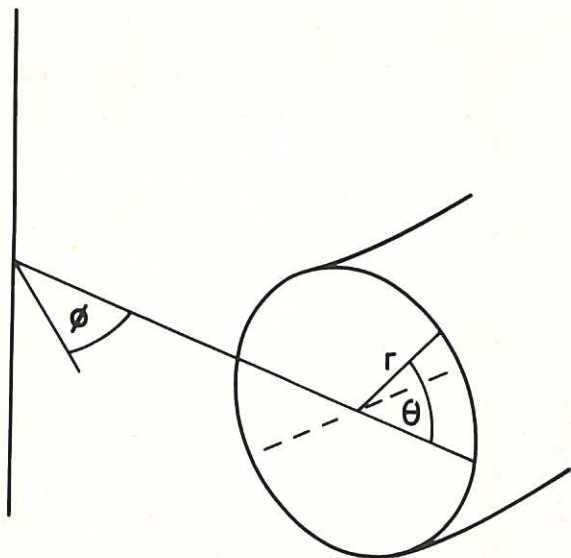


Fig.3.1 Toroidal co-ordinate geometry.

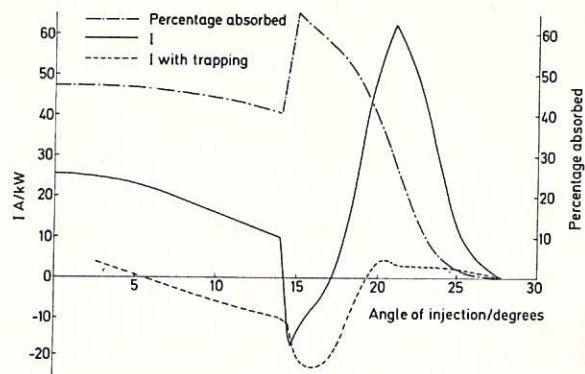


Fig.3.2 TOSCA, current and absorbed power versus ψ for 28 GHz, $\ell=2$, $n_e(0) = 4 \times 10^{18} \text{ m}^{-3}$ and $T_e(0) = 500\text{eV}$.

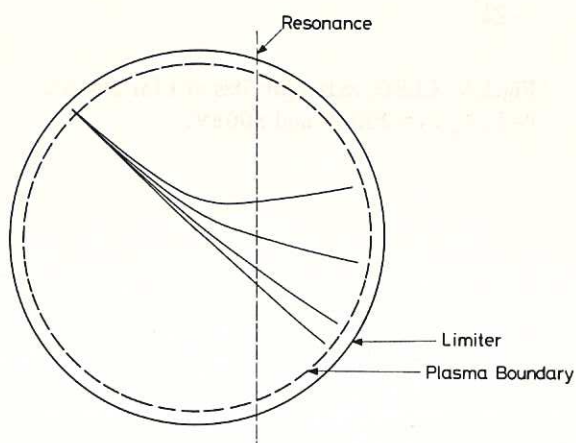


Fig.3.3 TOSCA, radial profiles of I for $T_e(0) = 500\text{eV}$ and 1 keV.

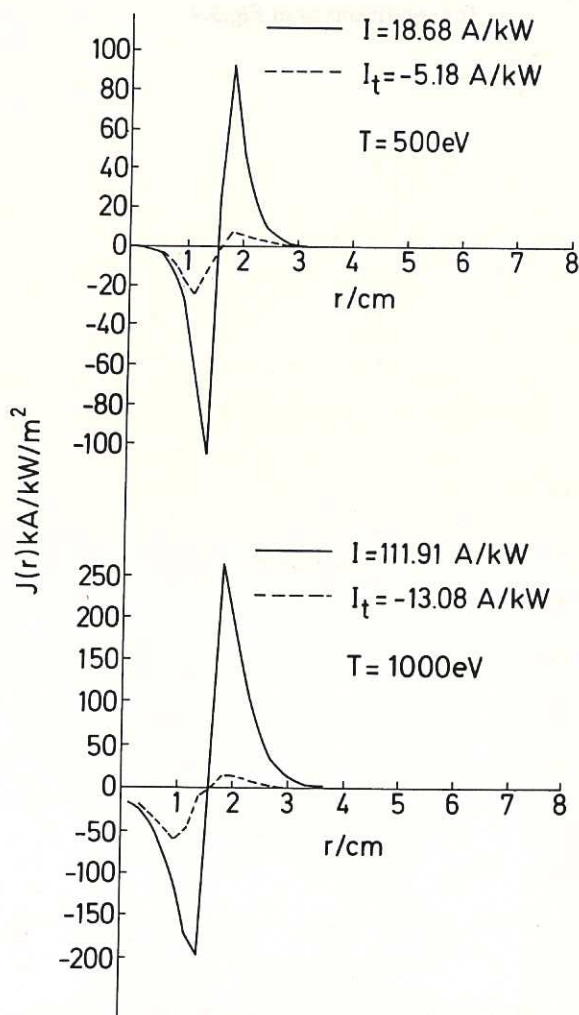


Fig.3.4 CLEO, ray trajectories projected onto minor cross section for 28 GHz, $\ell=1$, $n_e(0) = 10^{19} \text{ m}^{-3}$, $T_e(0) = 200\text{eV}$ and $B(0) = 1.05\text{T}$.

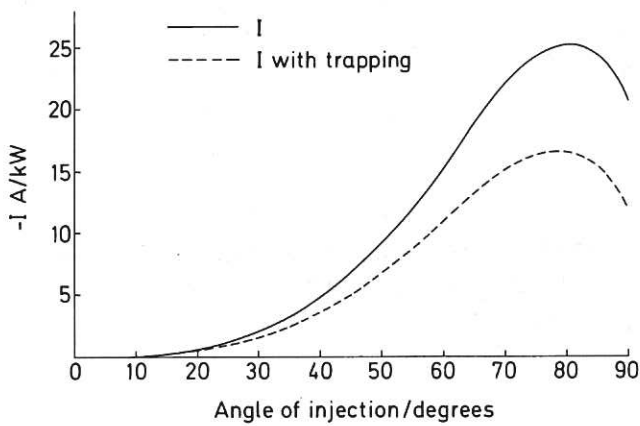


Fig.3.5 CLEO, current versus ψ for conditions as in Fig.3.4.

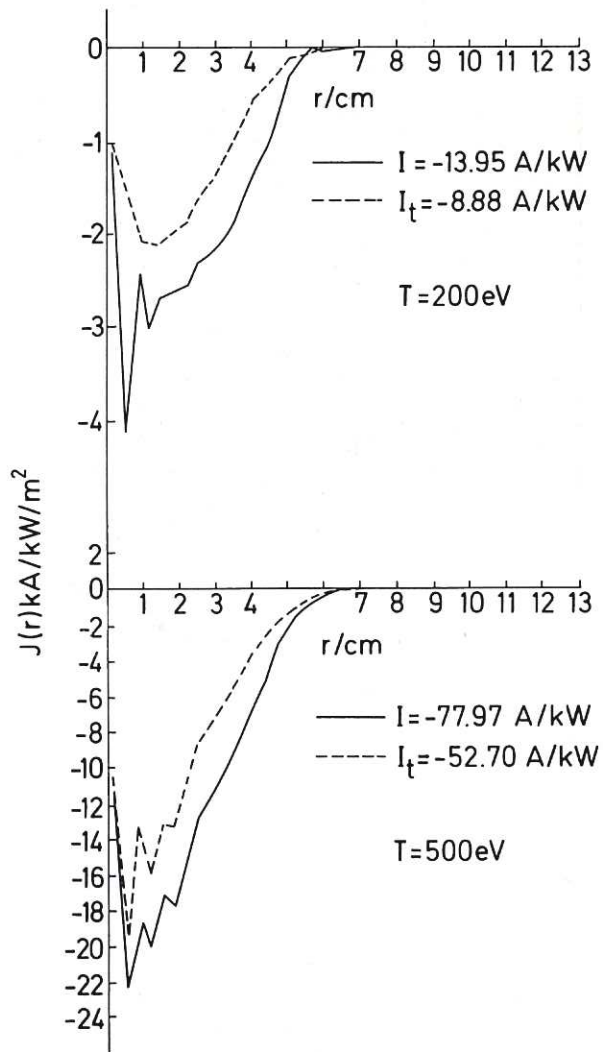


Fig.3.6 CLEO, radial profiles of I for 28 GHz, $\ell=1$, $T_e(0) = 200\text{eV}$ and 500eV .

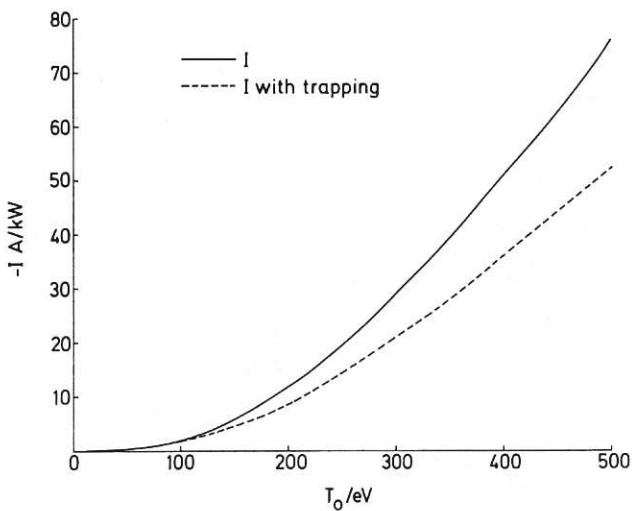


Fig.3.7 CLEO, current versus $T_e(0)$ for $\psi=55^\circ$ with other conditions as in Fig.3.4.

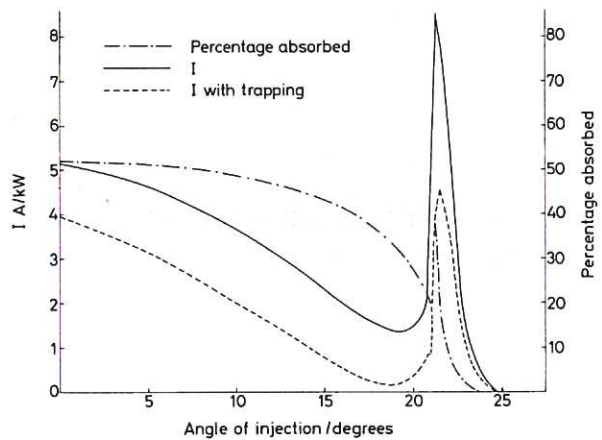


Fig.3.8 CLEO, current and absorbed power versus ψ for 28 GHz, $\ell=2$, $n_e(0) = 4 \times 10^{18} \text{m}^{-3}$, $T_e(0) = 200\text{eV}$ and $B(0) = 0.5\text{T}$.

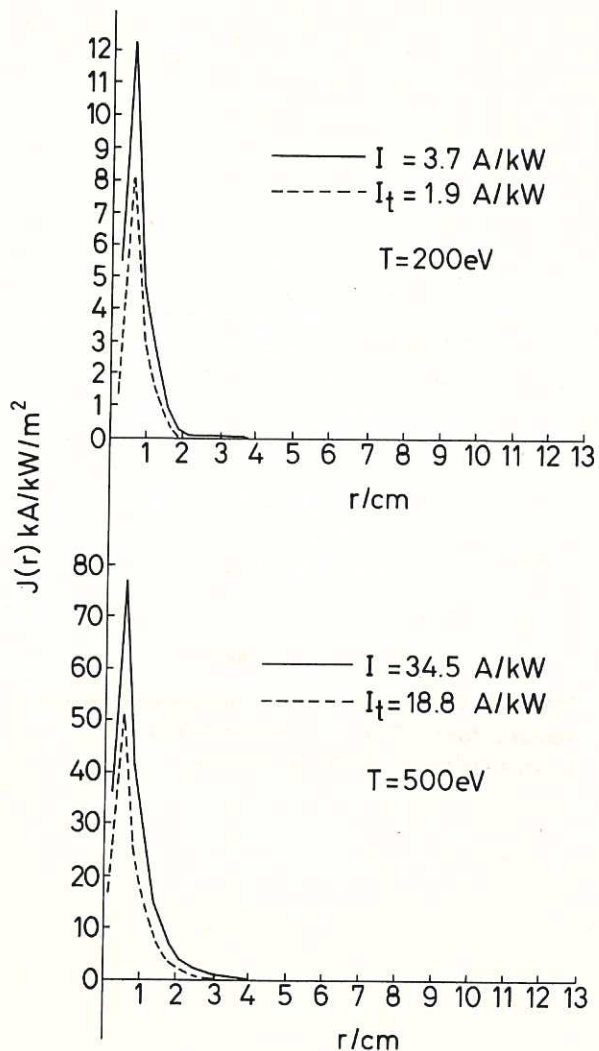


Fig.3.9 CLEO, radial profiles of I for 28 GHz, $\ell=2$, $T_e(0) = 200\text{eV}$ and 500eV .

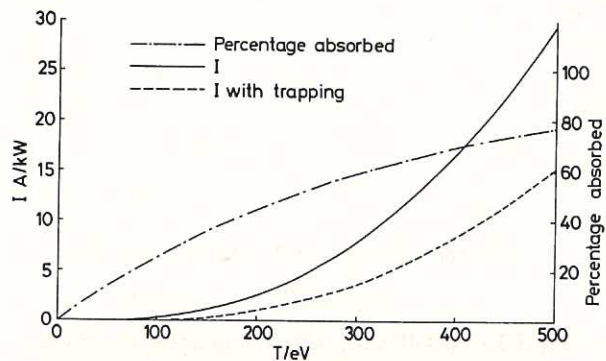


Fig.3.10 CLEO, current and absorbed power versus $T_e(0)$ for $\psi=14^\circ$ with other conditions as in Fig.3.8.

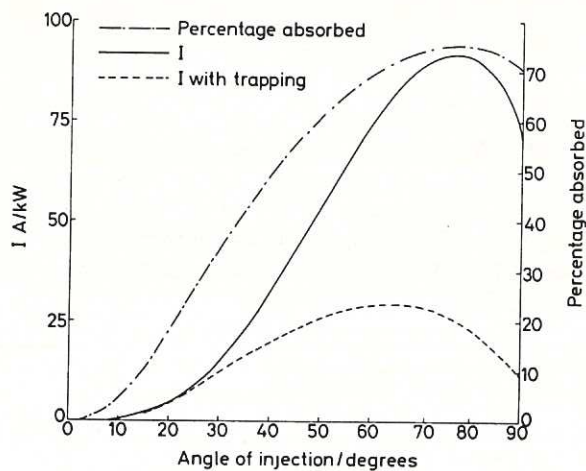


Fig.3.11 COMPASS, current and absorbed power versus ψ for 28 GHz, $\ell=1$, $B(0) = 1.05\text{T}$, $n_e(0) = 10^{19}\text{m}^{-3}$ and $T_e(0) = 800\text{eV}$.

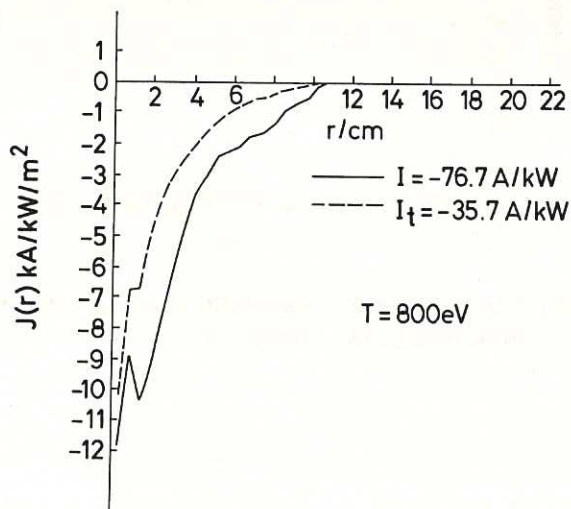


Fig.3.12 COMPASS, radial profile of I for conditions as in Fig.3.11 and $\psi=60^\circ$.

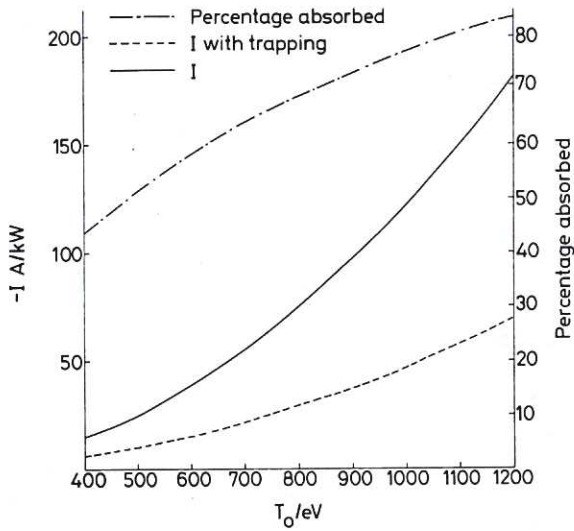


Fig.3.13 COMPASS, current and absorbed power versus $T_e(0)$ for $\psi=60^\circ$ and other conditions as in Fig.3.11.

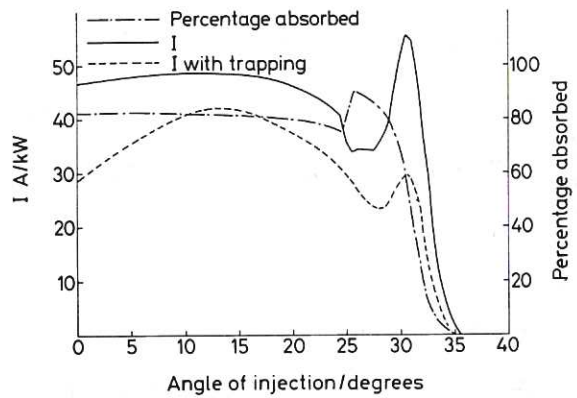


Fig.3.14 COMPASS, current and absorbed power versus ψ for 60GHz, $l=2$ $B(0) = 1.05$ T, $n_e(0) = 10^{19} \text{ m}^{-3}$ and $T_e(0) = 800 \text{ eV}$.

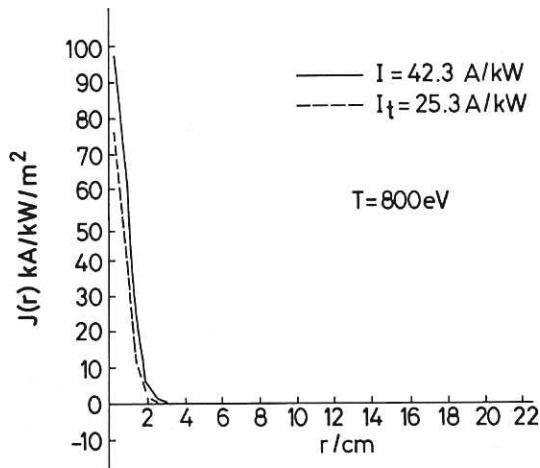


Fig.3.15 COMPASS, radial profile of I for $\psi=20^\circ$ and other conditions as in Fig.3.14.

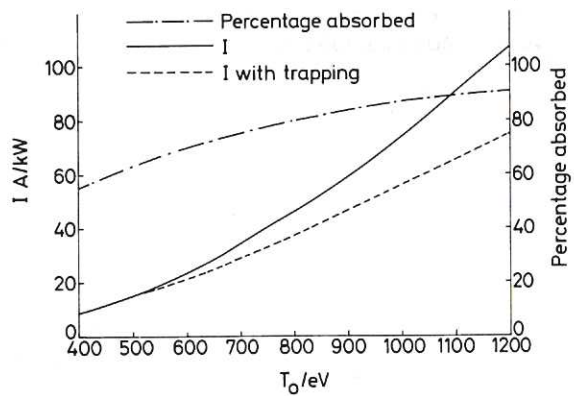


Fig.3.16 COMPASS, current and absorbed power versus $T_e(0)$ for $\psi=20^\circ$ and other conditions as in Fig.3.14.

4. USES OF ELECTRON CYCLOTRON RESONANCE HEATING ON DITE

W H M Clark and J Hugill

At present, the DITE experiment employs up to 2.4MW of neutral beam injection for the study of (a) plasma confinement at higher temperature and β , (b) beam-driven currents and (c) the extension of the regime for stable operation in $I \nu \bar{n}_e$ parameter space. The present availability of high power 'gyrotron' oscillators for ECRH prompts us to ask how these could be used to assist this programme. Compared with neutral beams, ECRH offers advantages: energy deposition is more local and therefore more controllable, no neutrals are deposited deep inside the plasma, which can give rise to unwanted side effects, and geometrical requirements for conveying the power to the torus are simplified.

This paper compares the regions in parameter space which are accessible with ohmic heating, neutral beam injection and ECRH at 60GHz and outlines a possible physics programme.

4.1 ACCESSIBILITY

The requirement for accessibility of the resonance zone to waves launched in free space, outside the plasma column, imposes restrictions on the plasma density. Five cases are considered: the fundamental 0-mode launched from either the outside ($f > f_{ce}$) or the inside ($f < f_{ce}$) of the plasma column, the second harmonic X-mode (X_2) launched from the outside or inside and the fundamental X-mode (X_1) launched from the inside.

The density and temperature profiles are modelled by the forms:

$$n_e = n_{e0}(1 - r^2/a^2), T_e(\text{keV}) = 0.8(1 - r^2/a^2)^p, q_L = 1 + \frac{3}{2} p, \quad (1)$$

the latter giving $q_0 \sim 1$ with $j \sim T_e^{3/2}$. The maximum line average densities, $\bar{n}_e = \frac{2}{3} n_{e0}$ are calculated for resonance at the centre of the discharge ($q = 1$) and at the $q = 2$ surface, these being the locations of most interest for the programme outlined below. The critical densities calculated for these various conditions are shown in Fig. 4.1 in a plot of $\frac{1}{q_L} \nu M (= \bar{n}_e R_0/B_{T0})$ for a wave frequency, $f = 60\text{GHz}$, corresponding to

$B_{T0} = 1.66$ to $2.62T$ for $f = f_{ce}$ and $B_{T0} = 0.83$ to $1.3.T$ for $f = 2f_{ce}$. Also shown on Fig 4.1 are the densities where the optical depth, $\tau = 1$ for perpendicular propagation, τ being given by [20]:

$$\tau = \frac{\pi^2 R}{\lambda} \left(\frac{T(\text{keV})}{511} \right) X (1 - X)^{1/2} \text{ for the O-mode}$$

$$\tau = \frac{4\pi^2 R}{\lambda} \left(\frac{T(\text{keV})}{511} \right) X (1 - 2X)^{1/2} \left\{ \frac{3 - 2X}{3 - 4X} \right\}^{5/2} \text{ for the } X_2\text{-mode} \quad (2)$$

where $X = n_e / 4.47 \times 10^{19} \text{ m}^{-3}$.

Figure 4.1 also shows the regions in parameter space where stable tokamak discharges are obtained in DITE, with ohmic heating only, and with the application of neutral beam injection at up to 1MW [21]. Evidently, most of the stable region can be explored by one of the five cases discussed above, each having its own advantages for particular applications.

4.2 APPLICATIONS

4.2.1 BULK ELECTRON HEATING

Application of $P_{rf} \geq P_{OH}$ can be expected to produce a substantial increase in T_e and relatively much smaller changes in T_i and \bar{n}_e , as on ISX [2] and T-10 [22], allowing the temperature scaling of electron transport to be studied, though in a restricted parameter range so far as B_T and \bar{n}_e are concerned.

The presence of anisotropic and/or non-Maxwellian distributions in velocity space can be detected by their effect on radial equilibrium [23] and by soft X-ray spectroscopy, supplemented by arrays of soft X-ray diodes.

In conjunction with neutral beam injection, ECRH could also aid our understanding of the beam driven current in at least two ways.

- a) by heating electrons, thus increasing the slowing down time and hence the stacking of fast ions,
- b) by increasing the proportion of trapped electrons [10,12], whose effect on the beam driven current has yet to be established. A combination of ECRH and NBI may allow beam driven current in a pure plasma.

4.2.2 BULK CURRENT DRIVE

Current drive by ECRH itself also appears possible (ref [16] and section 5) and the DITE Group is in a good position to exploit its experience in this area following the successful demonstration of current drive by NBI.

For bulk electron heating and current drive, resonance near the centre of the torus is desirable. The X_1 mode, launched from the inside, obviously allows operation at higher density, but the relative simplicity of launching the 0 or X mode from the outside makes them more desirable for the current drive experiments, for which low plasma densities are in any case used.

4.2.3 PROFILE CONTROL

Because it is resonant, ECRH can be used to deposit energy locally and hence to modify both the power deposition profile, $p_{rf}(r)$ and the profile of the electromotive force due to wave-particle interactions, $e(r)$. In principle this allows local modifications of T_e , T'_e , j and j' . Three areas of study are of interest for the DITE programme:

- a) the effect of local variations in T_e and T'_e on electron conduction;
- b) the effect of changes in p' and j' on the stability of tearing modes, particularly the $m = 2$, $n = 1$ mode, which appears to be the main precursor to disruption, and
- c) the effect of changes in T_e on the heat and particle transport in the scrape-off layer of diverted discharges.

Changes in $j(r)$ can arise directly from rf driven current or indirectly via electron heating [24]. In either case the time scale for the establishment of a quasi-steady current profile depends on the plasma conductivity. It is relatively rapid near the $q = 2$ surface, where the plasma temperature is low. Rf driven currents should be particularly effective for flattening the current profile in cases where oppositely directed emfs are produced on either side of the resonance layer. By contrast, the electron temperature profile can only be flattened temporarily by rf power levels in excess of the power conducted outwards from the discharge centre, unless gradients in the poloidal direction are admitted.

Figure 4.1 shows that a large part of the parameter space of present experiments can be accessed by the various cases discussed in section 1. In particular, for resonance at $q = 2$ near the high density limit the X_1 mode is appropriate, though the optical depth is very small, unless mode conversion occurs. For low- q_L operation, the X_2 mode injected from the outside of the torus has the greatest optical depth.

4.3 CONCLUSIONS

Application of ECRH to the DITE experiment could significantly improve our understanding of electron transport, both in the discharge core and the periphery, and of beam and rf driven current. The stabilising effect on the $m = 2$ mode may allow operation at lower q_L and/or higher densities than previously obtained. The power level required for studying critical β is up to several MW (see section 2) but useful work on other aspects of the programme could be done with $P_{rf} \geq P_{OH}$ ($\sim 200\text{kW}$).

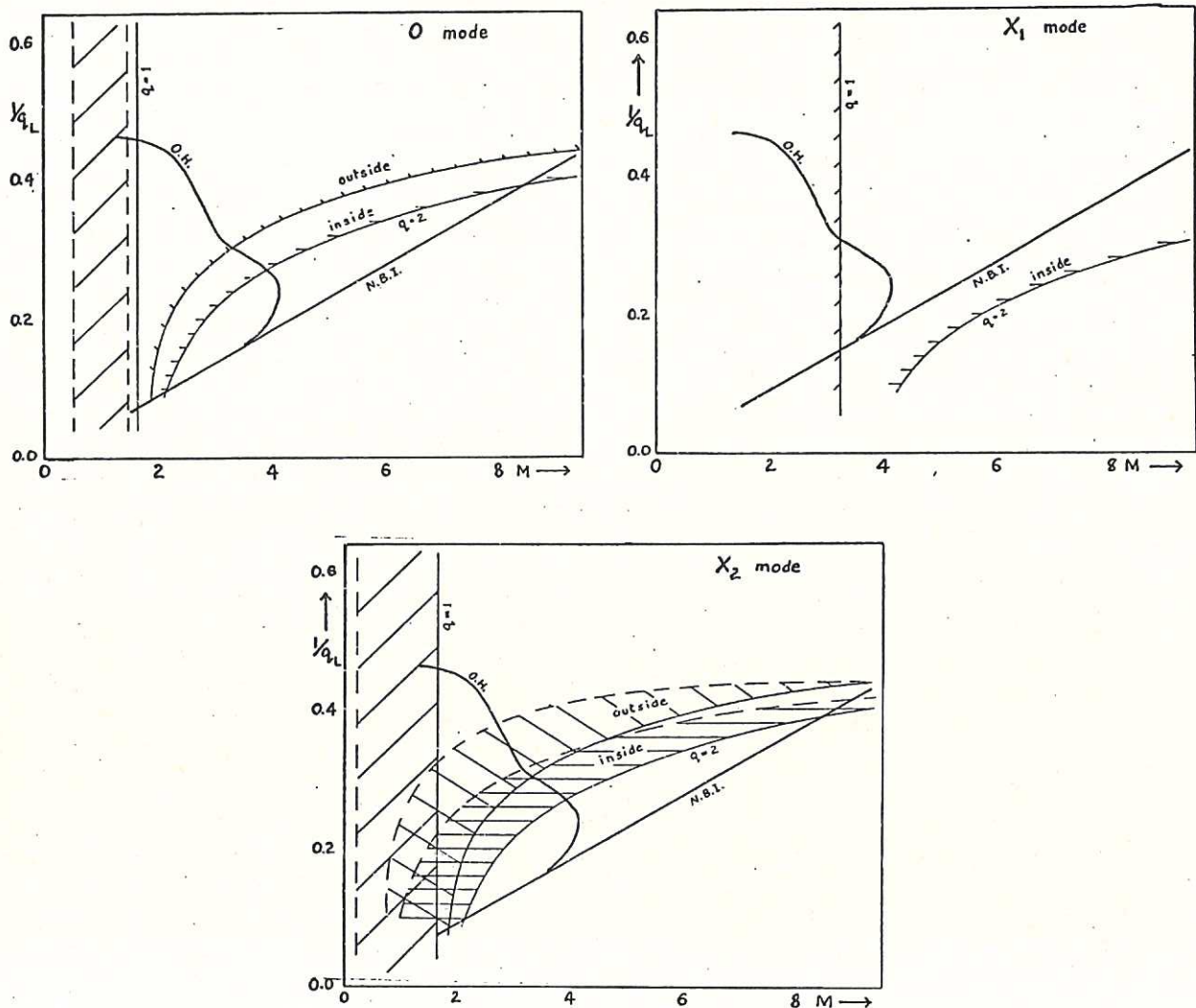


Fig.4.1 Shows density limits in $1/q_L$ v M space for ohmically heated (OH) and neutral beam injection heated (NBI) discharges in DITE. Superimposed are positions of cut-offs (solid lines) and $\tau = 1$ (dotted lines) for the various cases discussed in the text for resonance at $q = 1$ (centre) and $q = 2$ surfaces. Conditions - $f = 60$ GHz, $n_e = n_{e0}(1 - r^2/a^2)$, $T_e = 0.8(1 - r^2/a^2)^p$, $q_L = 1 + 3/2 p$, $R_0 = 1.17$ m and $a = 0.26$ m.

5. CURRENT DRIVE AND PROFILE CONTROL WITH ECRH ON DITE by C N Lashmore-Davies, R A Cairns and J Owen

5.1 INTRODUCTION

DITE is a large enough tokamak to carry out an interesting range of electron cyclotron heating experiments with the O-mode at a frequency of 60GHz. Such a programme would be a very timely test bed for a possible future application of ECRH to JET. Some of the experiments that could be carried out relate to current drive, profile control and if sufficient power could be provided at 60GHz, bulk heating. The DITE operating range, discussed by Clark and Hugill (see Sec. 4), shows that in order to perform some of the more interesting ECRH experiments some bulk heating will probably be required. Most of the discussion given in this paper will focus on the O-mode at the fundamental although we shall also mention the X-mode. The optical depth τ of the O-mode at the fundamental is given by⁽²⁰⁾

$$\tau = 2.3 \times 10^{-2} \times R(\text{m}) \times f(\text{GHz}) \times T_e(\text{keV})$$

which refers to the optimum density for absorption where $\omega_p^2/\Omega^2 = 2/3$. In order to have an absorption coefficient of 80% for DITE at 60GHz a density of $3 \times 10^{19}/\text{m}^3$ and a temperature of 1keV is required. These conditions could be obtained at the centre of the discharge but, at present, could not be achieved at the $q = 2$ surface (say). In order to achieve sufficient optical depth in the vicinity of the $q = 2$ surface the temperature would have to be raised to 1keV. For existing DITE conditions the second harmonic X-mode would be more appropriate. In the remainder of this paper, we shall be concerned with current drive and control of the current profile.

5.2 CURRENT DRIVE

Present experimental evidence for current drive with ECRH has been attributed to the X-mode either at the fundamental⁽¹⁶⁾ or the second harmonic⁽⁷⁾. To date, current drive by means of the O-mode has not been reported. Such an experiment, however, appears feasible on DITE. Although the DITE plasma may not be optically thick current drive could still be effective with the O-mode due to the relativistic corrections to the resonance condition⁽¹⁹⁾. These effects introduce an asymmetry such that the current does not reverse sign as the wave passes through the resonance for small values of n_z ($n_z = ck_z/\Omega$). The asymmetry can be most easily

seen if the resonance condition with the relativistic correction included is solved for v_z , where v_z is the component of the electron velocity along the equilibrium magnetic field. The result is illustrated in figure 5.1 and shows, amongst other things, that current drive depends strongly on whether the wave is launched from the low field or the high field side.

The calculation of the current driven by the O-mode at the fundamental shows a number of features which require experimental verification. These currents were calculated with the Lorentz gas model^(16,19) using a simplified collision term. Such a calculation overestimates the current. The calculations of Cordey et al.⁽¹⁶⁾ show that a full Fokker-Planck treatment reduces the value of the ratio of current to power absorbed by a factor 6. With the aid of a result of Fisch et al.⁽¹⁴⁾ we have been able to show that the ratio of current to power obtained from the Lorentz gas model is larger than the corresponding quantity obtained from the Fokker-Planck model by the quantity $(5 + Z_i)/Z_i$ in agreement with Cordey et al.⁽¹⁶⁾. The calculations given in this paper relate to the Lorentz model and must therefore be reduced by a factor 6 for $Z_i = 1$.

Let us now consider two examples of current drive relevant to DITE. These are shown in figures 5.2 and 5.3. Figure 5.2 is a plot of the current and power density profiles for the O-mode propagating through the resonant layer from the low field side for a value of $n_z = 0.1$. The units of current and power in figures 5.2 and 5.3 are arbitrary and illustrate the variation of these quantities through the resonance region. For these calculations a major radius of 1.2m was assumed, a temperature of 1keV, a density corresponding to $\omega_{pe}^2/\Omega^2 = 0.75$ and a wave frequency of 60 GHz. Notice that the current does not reverse its direction of flow at any point in the resonance region. Figure 5.3 shows a similar plot for $n_z = 0.3$. For this case there is a reversal of the current as the wave passes from the low field side of the resonance to the high field side. This was to be expected since as n_z increases the relativistic effects become weaker. The variation of the ratio of total current integrated through the resonance layer to the total power absorbed as a function of n_z is shown in figure 5.4 for the same parameters as were used in figures 5.2 and 5.3. The ratio of the current to power has been divided by the factor 6 so that the value plotted relates to $Z_i = 1$ and represents the full Fokker-Planck value. The current to power ratio reaches a maximum for a value of $n_z \approx 0.1$ and then falls away. This behaviour is evidently characteristic of a medium size tokamak such as DITE where the

absorption is fairly strong but not complete. The existence of this optimum angle for current drive with the O-mode from the low field side is a phenomenon which requires experimental verification.

Another point which would be very interesting to check experimentally is the strong dependence of the driven current on which side of the resonance the wave is launched. This dependence is a result of the relativistic correction to the resonance condition and shows that current drive is more effective from the high field side than from the low field side due to the wave encountering the more energetic particles first when it comes from the high field side. This is illustrated in figure 5.5 which was obtained for parameters relevant to JET. Figure 5.5 shows the ratio of the total current flowing through the resonant layer to the total power absorbed in the layer as a function of n_z . The ratio obtained from the Lorentz model has again been divided by 6 so that figure 5.5 is effectively the Fokker-Planck value for $Z_i = 1$. The O-mode is shown incident from the high and low field sides and the X-mode incident from the high field side is shown for comparison. It can be seen that the X-mode is the most efficient for current drive followed by the O-mode from the high field side. The ratio of the current driven by the O-mode from high and low field sides is approximately 1.5.

Experiments from the high field side on tokamaks not specifically designed with this in mind can be difficult. An interesting alternative to a high field side experiment would be to launch waves from the low field side of the resonance but where the conditions are chosen such that the wave frequency is everywhere less than the electron cyclotron frequency. By this means, the wave could couple to the more energetic electrons, a characteristic of current drive from the high field side. The currents produced would be in the outer layers of the plasma but this might be relevant to control of the current profile.

5.3 PROFILE CONTROL

With the realization⁽¹⁴⁾ that electron cyclotron waves can be as efficient as other forms of radio frequency heating for current drive, the possibility of controlling the current profile in a tokamak can be viewed from two points of view. The profile may be modified indirectly by producing a local increase in T_e or directly by driving a current locally.

A theoretical comparison of these two approaches will be made with a view to the guidance of future experiments.

The current drive experiments described in section 5.2 would require control over the polarization and launching angle necessary for the profile control application. Experiments of this type appear feasible on DITE. Although local heating can be achieved under conditions of weak absorption, for the present comparison high single pass absorption is required. For the present DITE operating conditions this only appears likely close to the plasma centre. Therefore, in order to explore this route to profile control, bulk electron heating might be required. It is also possible that if the CLEO experiment is able to operate at a magnetic field of 2 tesla then some of these experiments could be performed on CLEO as well.

For both of these concepts of profile control, it is expected that the relativistic corrections to the resonance frequency will be important since these effects can alter the location of the driven currents and the absorbed power.

5.4 CONCLUSIONS

The above programme of experiments on current drive, profile control and heating with the 0-mode at 60GHz (the fundamental on DITE) would be extremely relevant to a possible future application of ECRH to JET and other large tokamaks. The experience gained regarding efficient launch of the 0-mode polarization and control of the parallel refractive index n_z are directly applicable to these larger devices. In particular, information gained from profile control experiments is needed for the INTOR work and might also be useful to JET.

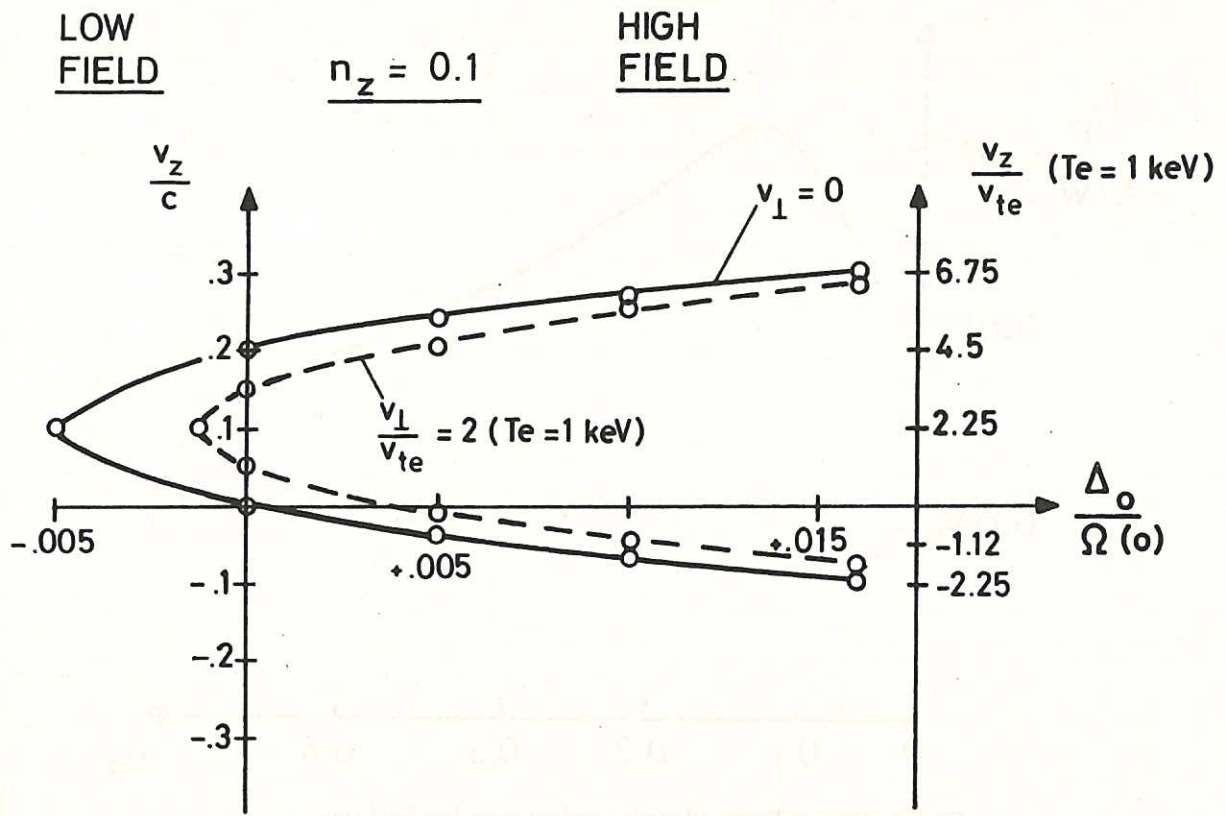


Fig.5.1 Where $\Delta_0 = \Omega(x) - \omega$.

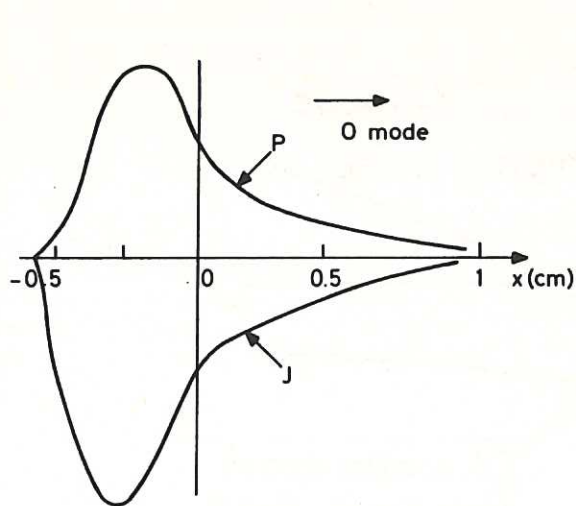


Fig.5.2 Power and current profiles for $n_z = 0.1$.

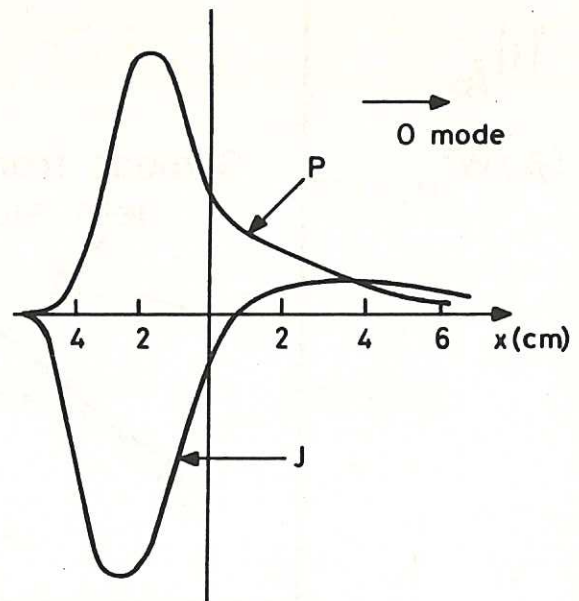


Fig.5.3 As Fig.5.2, $n_z = 0.3$.

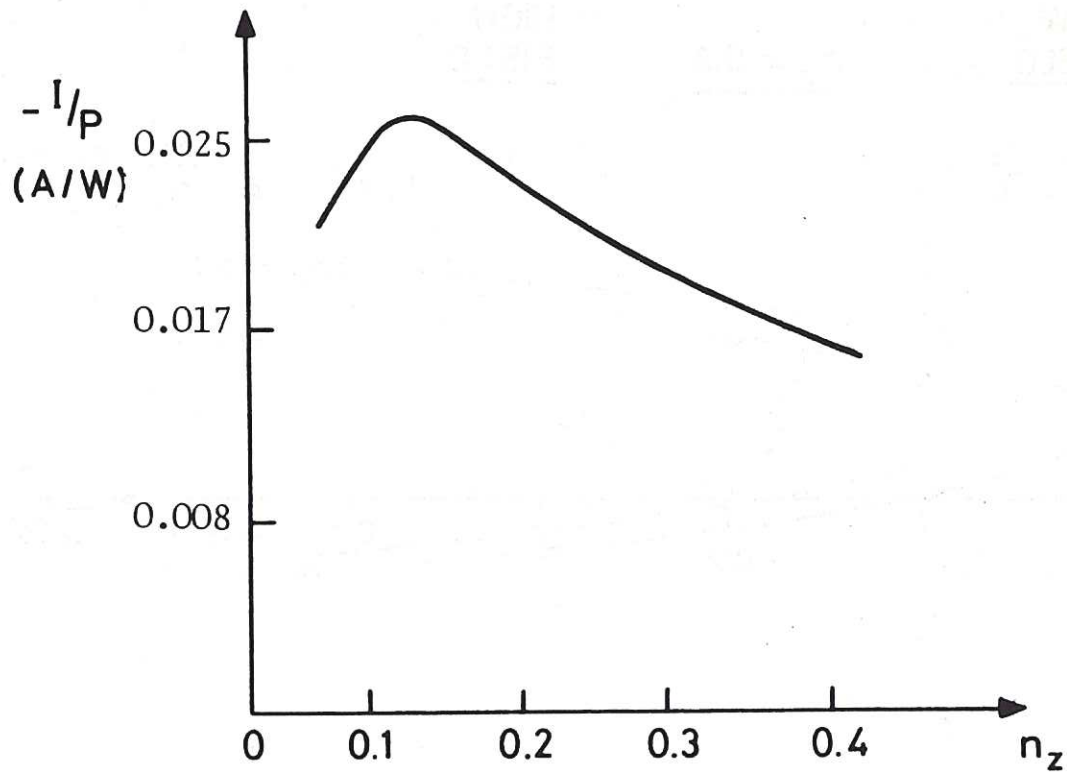


Fig.5.4 Current/Power (0 mode incident from low field side).

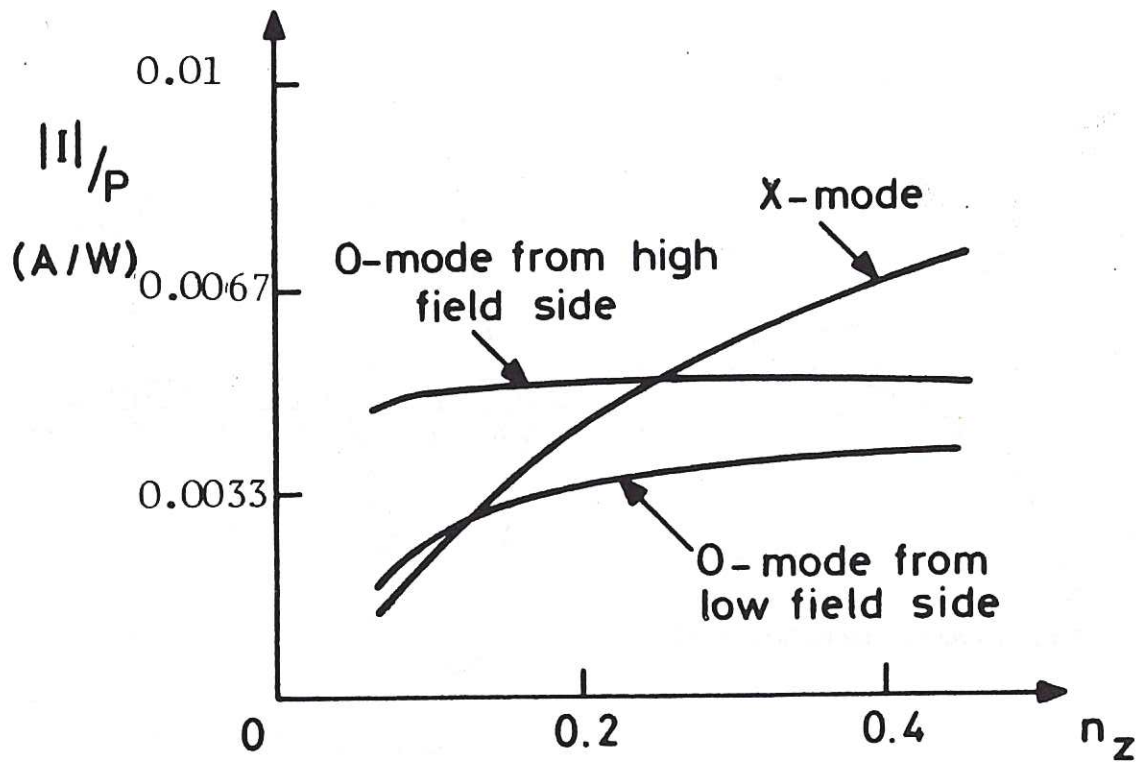


Fig.5.5 Current/Power as a function of n_z .

6. GYROTRON NEEDS AND WAVEGUIDE COMPONENTS

A C Riviere

Two 28 GHz gyrotrons have been in use for the last two years on the TOSCA and LEVITRON experiments and on a component test stand. These gyrotrons are expected to provide the power needed for the TOSCA, CLEO and COMPASS work at this frequency but a further 28 GHz tube may be needed as a replacement in case of a failure in one of the existing tubes.

Operation at a higher frequency is needed to allow studies in higher density plasmas. The purchase of one 60 GHz tube is planned for this year for work on TOSCA and CLEO, and further 60 or 70 GHz tubes will be needed during the years 1983 to 1985 to supply the power needed for the DITE and COMPASS work. Some enhancement of the power supplies will be needed for long pulses and for high power operation.

In the more distant future, 1986-1987, operation on DITE at the second harmonic and still higher densities will require gyrotrons in the 90/140 GHz frequency range. The overall pattern of demand is summarised in the Table, but note that, at the present time, only the purchase of the first of these is approved.

GHz	1982	1983	1984	1985	1986	1987
28		1 spare				
60/70	1	2	3	2 + 1 spare		
90/140					4	4

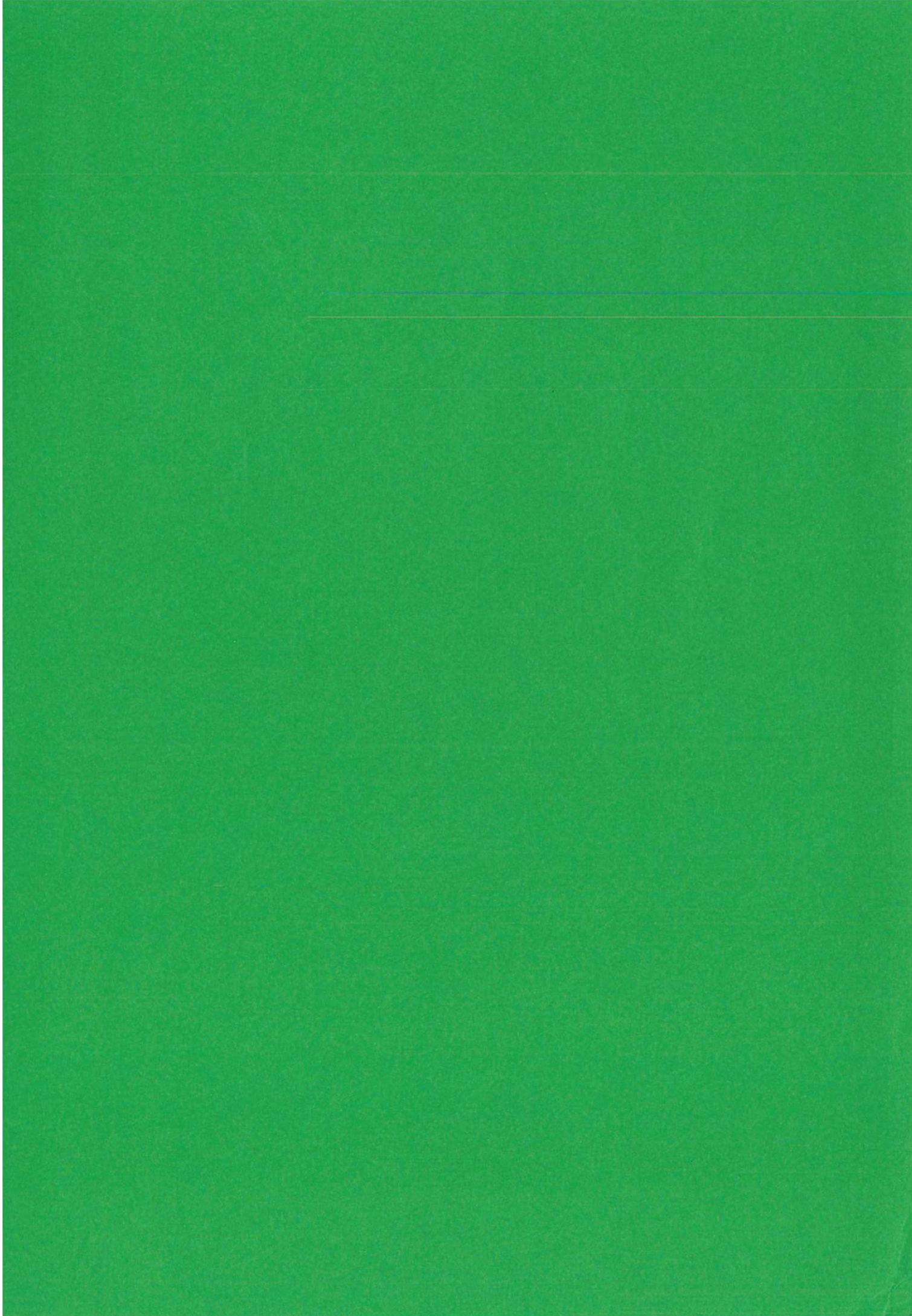
In principle very efficient transmission of the wave power from gyrotron to torus can be achieved by using circular electric modes in circular guide. This assumes perfect construction of the waveguide system but some imperfections are inevitable and these lead to mode conversion into modes with much higher attenuation. The mode conversion loss process increases as a function of a/λ where $2a$ is the guide internal diameter and λ is the vacuum wavelength. At sufficiently large a/λ however the concept of "guided waves" is weak and better transmission may be achieved with optical techniques. Our needs cover the range of a/λ from ~ 3 to ~ 15 (28 to 120 GHz) beginning in a truly "guided" wave

regime but ending in an almost optical regime. This implies the use of unconventional waveguide components which can be designed but do require significant development effort. A programme of work for the 28 GHz systems is being pursued at Culham to provide mode filters, power monitors, bends, mode convertors and antennae. This will be extended to the 60 GHz frequency range during 1983 with the delivery of the first 60 GHz gyrotron.

REFERENCES

- [1] V V Alikhaev et al, Sov. Phys. JETP Letts 15 (1972) 27;
V V Alikhaev et al, Sov. Jrnl of Plasma Phys. 2 (1976) 212;
V E Golant et al, Sov. Phys. Tech. Phys. 17 (1972) 488
- [2] R M Gilgenbach et al, Phys Rev Letts, 44 (1980), 647
- [3] R J La Haye et al, General Atomic Report GA-A16109, Oct 1980
- [4] B Lloyd et al, ECRH and ECE Workshop, Oxford 1980, pp 275;
B Lloyd et al, Proc 2nd Joint Int. Symp. on Heating in Toroidal Plasmas, Como, 1980, 1 181;
D C Robinson, Bull.Am.Phys. Soc. Vol 25, No.8 1980 pp 942;
M W Alcock et al, 10th Euro Conf on Contr. Fus. and Plasma Physics, Moscow 1981, "Local Heating and Current Drive Investigations on TOSCA";
M W Alcock et al ibid "High Power ECRH at the Second Harmonic in TOSCA!"
- [5] P J Lomas et al, 10th Euro Conf on Controlled Fusion and Plasma Physics Moscow 1981, Vol 1, A1a.
- [6] K McGuire et al, Proc of 8th Int. Conf. on Plasma Physics and Controlled Nuclear Fusion Res. (IAEA Vienna 1979) held at Innsbruck. Vol.1, p 335.
- [7] D C Robinson, Proc. 3rd Joint Varenna-Grenoble Int. Sym on Heating in Toroidal Plasmas, Grenoble 1982, paper E3.
- [8] L C Bernard et al, Phys Rev Letts 46 (1981) 1286
- [9] S Ejima et al, General Atomic Report, GA-A16497, 1982.
- [10] P J Fielding, Culham Laboratory Report, CLM-P615, 1980.
- [11] P J Fielding, Workshop on ECE and ECRH, CLM-ECR (1980) p 69.
- [12] M W Alcock et al, Proc. 10 th Euro Conf. on Controlled Nuclear Fusion and Plasma Physics, Moscow 1981, H15.
- [13] J J Ellis et al, 9th Int. Conf. Plasma Phys. and Contr. Nuc. Fus. Brussels 1980, IAEA Vienna, Vol. 1, p 731.
- [14] N J Fisch and A H Boozer, Phys.Rev.Letts 45 (1980) 720.
- [15] D F H Start et al, Phys.Rev.Letts 48 (1982) 620.
- [16] J G Cordey, T Edlington and D F H Start, Plasma Physics 24 (1982) 73.
- [17] D F H Start, J G Cordey and T Edlington to be published, also D F H Start, 3rd Joint Varenna-Grenoble Int. Symp on Heating in Toroidal Plasmas, Grenoble 1982.
- [18] M Bornatici, Proc. of Joint Workshop on ECE and ECRH, Oxford 1980, CLM-ECR (1980).
- [19] R A Cairns, J Owen and C N Lashmore-Davies, 3rd Joint Varenna-Grenoble Int. Symp on Heating in Toroidal Plasmas, Grenoble 1982.
- [20] T M Antonsen and W M Manheimer, Phys.Fluids 21 (12) 2295, (1978).
- [21] K B Axon et al, Plasma Physics and Controlled Nuclear Fusion Research, (Proc. 8th Int. Conf. Brussels, 1980), Vol I, IAEA, (1981) 405.

- [22] V V Alikaev et al, Controlled Fusion and Plasma Physics, (Proc. 10th Euro. Conf, Moscow, 1981), Vol.1, Moscow, (1981), H3.
- [23] W H M Clark et al, Phys. Rev. Letts 45, (1980), 1101.
- [24] V Chan, G Guest, Nuclear Fusion, 22, (1982) 272.



HER MAJESTY'S STATIONERY OFFICE

Government Bookshops

49 High Holborn, London WC1V 6HB
(London post orders: PO Box 569, London SC1 9NH)
13a Castle Street, Edinburgh EH2 3AR
41 The Hayes, Cardiff CF1 1JW
Brazennose Street, Manchester M60 8AS
Southey House, Wine Street, Bristol BS1 2BQ
258 Broad Street, Birmingham B1 2HE
80 Chichester Street, Belfast BT1 4JY

Publications may also be ordered through any bookseller